Bioorganic Chemistry 92 (2019) 103217

Contents lists available at ScienceDirect

Bioorganic Chemistry

journal homepage: www.elsevier.com/locate/bioorg

Design, synthesis, and molecular docking study of new piperazine derivative as potential antimicrobial agents

Mahadev Patil[a], Anurag Noonikara Poyil[b], Shrinivas D. Joshi[c], Shivaputra A. Patil[d], Siddappa A. Patil[a,*], Alejandro Bugarin[e,*]

[a] Centre for Nano & Material Sciences, Jain University, Jain Global Campus, Bangalore 562112, Karnataka, India
[b] Department of Chemistry & Biochemistry, University of Texas at Arlington, Arlington, TX 76019, USA
[c] Novel Drug Design and Discovery Laboratory, Department of Pharmaceutical Chemistry, S. E. T's College of Pharmacy, Sangolly Rayanna Nagar, Dharwad 580 002, Karnataka, India
[d] Pharmaceutical Sciences Department, College of Pharmacy, Rosalind Franklin University of Medicine and Science, 3333 Green Bay Road, North Chicago, IL 60064, USA
[e] Department of Chemistry and Physics, Florida Gulf Coast University, Fort Myers, FL 33965, USA

ARTICLE INFO

Keywords:
Piperazine derivatives
Synthesis
Characterization
Molecular docking
Antimicrobial activity

ABSTRACT

Herein, we describe the successful design and synthesis of seventeen new 1,4-diazinanes, compounds commonly known as piperazines. This group of piperazine derivatives (**3a-q**) were fully characterized by ^{1}H NMR, ^{13}C NMR, FT-IR, and LCMS spectral techniques. The molecular structure of piperazine derivative (**3h**) was further established by single crystal X-ray diffraction analysis. All reported compounds were evaluated for their antibacterial and antifungal potential against five bacterial (*Staphylococcus aureus, Escherichia coli, Klebsiella pneumoniae, Acinetobacter baumannii,* and *Pseudomonas aeruginosa*) and two fungal strains (*Candida albicans and Cryptococcus neoformans*). The complete bacterial screening results are provided. As documented, piperazine derivative **3e** performed the best against these bacteria. Additionally, data obtained during molecular docking studies are very encouraging with respect to potential utilization of these compounds to help overcome microbe resistance to pharmaceutical drugs, as explicitly noted in this manuscript.

1. Introduction

Bacterial and fungal infections are posing serious health threats globally in large part due to their increasing resistance to a large number of known antimicrobial drugs [1,2]. It is well known that microbes can develop resistance to pharmaceuticals by altering their target site, enzymatic resistance, and expression of efflux pumps. Drug efflux is particularly significant as it decreases drug uptake in the cells [3]. The ever-escalating drug resistance problem has encouraged medicinal chemists to design and develop novel drug candidates to help mitigate this problem. In this context, we have examined a variety of relatively small bioactive molecules for use as pre-clinical drug candidates. For example, we have previously examined potential pharmacophores such as chalcones [4], ureas [5], and *N*-heterocyclic carbene-metal complexes [6–13]. The present manuscript significantly extends our studies on this important research topic.

Nitrogen heterocycles remain an attractive topic for small molecular drug design and discovery. Among all heterocycles, piperazines, the six-membered nitrogen-containing heterocyclic ring, are certainly an

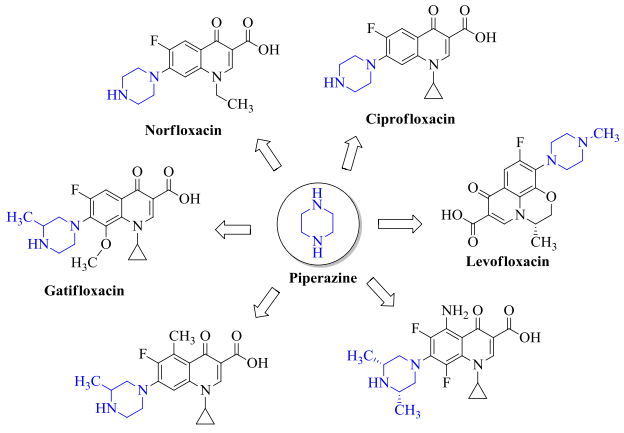

Fig. 1. Antibiotics containing piperazine moiety.

* Corresponding authors.
E-mail addresses: p.siddappa@jainuniversity.ac.in (S.A. Patil), abugarin@fgcu.edu (A. Bugarin).

https://doi.org/10.1016/j.bioorg.2019.103217
Received 17 July 2019; Received in revised form 19 August 2019; Accepted 22 August 2019
Available online 26 August 2019

established important pharmacophore in medicinal chemistry [14,15]. For example, the piperazine moiety is present in the core structure of many important commercial fluoroquinoline antibiotics such as: Norfloxacin, Ciprofloxacin, Gatifloxacin, Grepafloxacin, Sparfloxacin, and Levofloxacin [14] (Fig. 1). Of particular significance is the fact that combining the piperazine moiety with other heterocyclic ring systems, such as tetrazole, has resulted in new antifungal agents [15]. Such prior studies have clearly identified the potential use of piperazine derivatives as important pharmacophores.

Therefore, in continuation of our research efforts to identify novel new effective antimicrobial agents, we herein describe the design, synthesis, antimicrobial evaluation, and molecular docking of a wide range of new 1,4-di(hetero)aryl substituted piperazine analogs.

2. Result and discussion

2.1. Chemistry

The general synthetic approach employed to prepare these piperazine derivatives (**3a-q**) is outlined in Scheme 1 (for reaction optimization see the ESI). The starting materials for the synthesis of piperazine derivatives, namely: 1-benzhydrylpiperazine, 1-((4-fluorophenyl)(phenyl)methyl) piperazine, 1-((2-fluorophenyl)(4-fluorophenyl)methyl) piperazine and 11-(piperazin-1-yl)dibenzo[*b,f*][1,4] thiazepine were synthesized following published procedure [16,17], (also see the supporting information). All compounds (**3a-q**) were prepared in a simple, one-step reaction of previously prepared aryl isocyanates and mono-substituted piperazines in toluene at 40–45 °C. This method has the advantages of fast reactions (1 h), easier work-up, mild reaction conditions, and good yields (70–78%).

2.2. Spectroscopic characterization

The newly synthesized piperazine derivatives containing aryl moieties (**3a-q**) were characterized using IR, ^{1}H NMR,^{13}C NMR, and mass spectrometry. The spectral data of the newly synthesized compounds (**3a-q**) are detailed in the experimental section. The FT-IR spectra, for all derivatives, were recorded in the region from 4000 to 400 cm^{-1}, wherein the observed bands at 3356–3251 cm^{-1} were assigned to the ν(NH) groups of the urea moiety. The IR spectra of all derivatives show stretching frequencies around 1628–1707 cm^{-1}, which correspond to the ν(C═O) groups. Weak to medium absorptions, observed around 2814–2956 cm^{-1}, are assigned to the =C−H stretch of the aromatic ring. Structural information of the compounds was further established by using ^{1}H NMR and ^{13}C NMR spectra. The ^{13}C NMR spectra of these derivatives exhibit a signal characteristic of the (C═O) functional groups between 154.9 and 152.2 ppm.

2.3. X-ray crystallography

X-ray quality single crystals were obtained from recrystallization, in chloroform-*d* solution, of the N-(4-chlorophenyl)-4-(dibenzo[*b,f*][1,4] thiazepin-11-yl)piperazine-1-carboxamide (**3h**). The crystals provided a good diffraction pattern and thus an unequivocal molecular structure for this compound. The compound (**3h**) was found to crystallize in a monoclinic unit cell and $P2_1$ space group. The crystal structure of

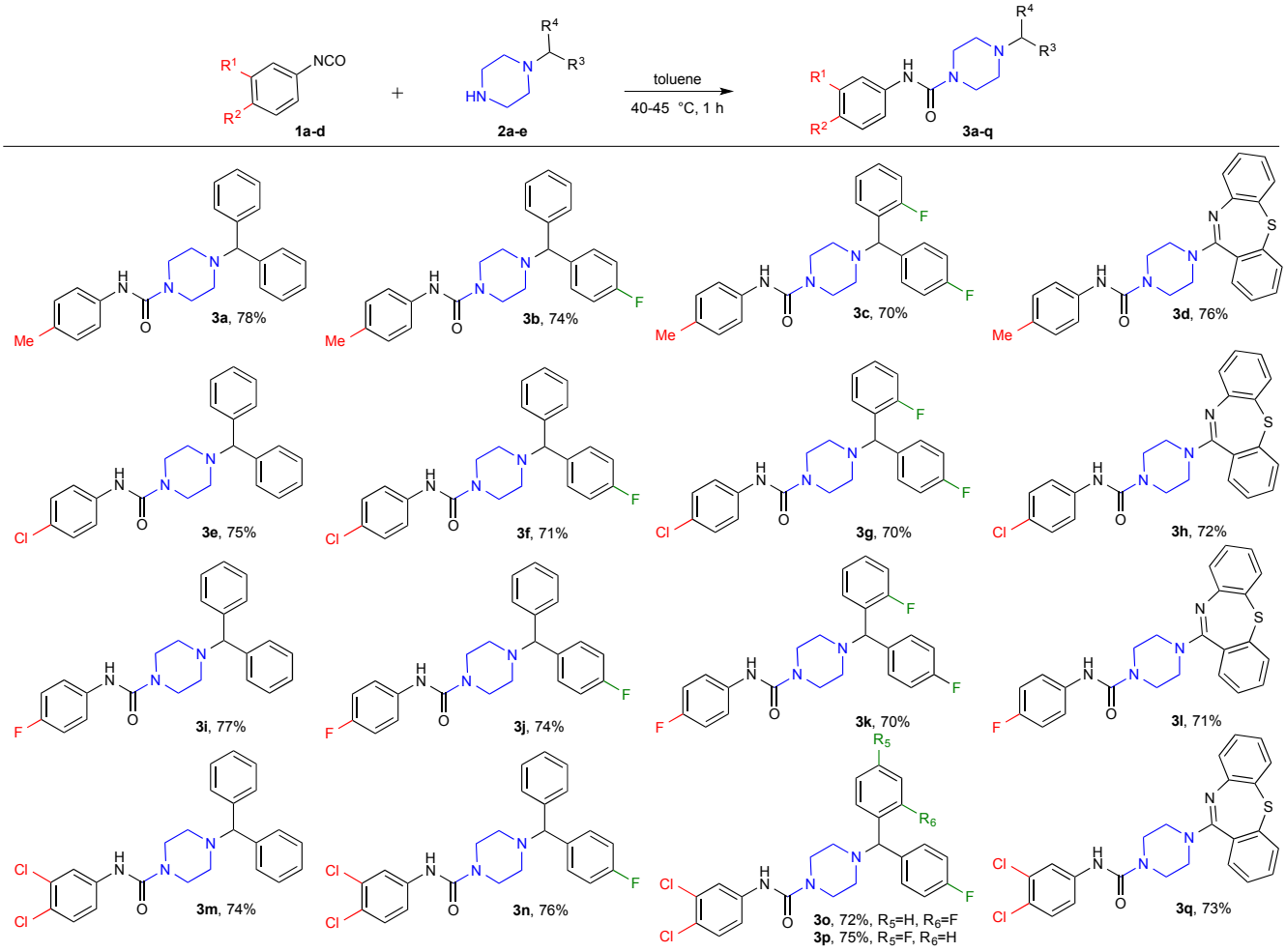

Scheme 1. Direct synthesis of disubstituted-piperazine derivatives.

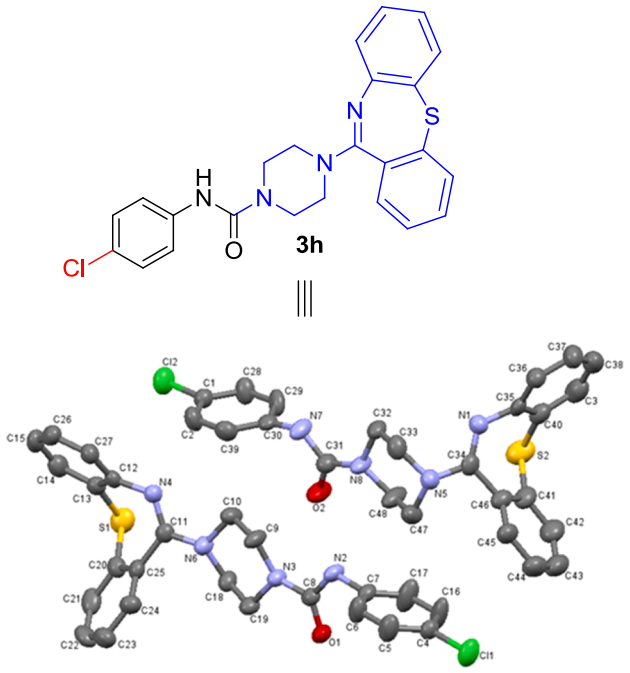

Fig. 2. X-ray diffraction structure of **3h**; molecule; thermal ellipsoids are drawn on the 50% probability level. Additional data check CCDC 1939260.

Table 1
Crystal data and structure refinement for **3h**.

Identification code	**3h**
Empirical formula	$C_{24}H_{21}ClN_4OS$
Molecular formula	$C_{24}H_{21}ClN_4OS$
Formula weight	449.0
Temperature	293 K
Crystal system	Monoclinic
Space group	$P2_1$
Unit cell dimensions	a = 6.1263(5) Å b = 37.4701(9) Å c = 9.5021(6)Å α = 90° β = 102.626(12)° γ = 90°
Volume	2128.49(7) Å^3
Z	4
Radiation type	Mo-Kα
Density (calculated)	1.4011 Mg/m^3
Absorption coefficient	0.303 mm^{-1}
F(0 0 0)	936
Crystal size	0.32 × 0.28 × 0.05 mm^3
Theta range for data collection	2.17 to 28.44°.
Index ranges	$-8 \le h \le 8$, $-49 \le k \le 49$, $-12 \le l \le 12$
Diffractometer Bruker SMART APEXII	Absorption correction multi-scan (SADABS; Bruker, 2014)
Reflections collected	10,550
Independent reflections	10,550 [R(int) = 0.0408]
Completeness to θ_{max}	99%
Max. and min. Transmission	0.908 and 0.985
Goodness-of-fit on F^2	1.30
Final R indices [I > 2sigma(I)]	R1 = 0.1321, w$R2$ = 0.0408
R indices (all data)	R1 = 0.0440, w$R2$ = 0.0509
ρmax,ρ min (e$^-$/Å^3)	0.27(e$^-$/Å^3), −0.25(e$^-$/Å^3)

Software: APEX2 and SAINT (Bruker, 2014) [18], SHELXS97 and SHELXL2013 (Sheldrick, 2008) [19], and JANA2006 [20].

compound (**3h**) is shown in Fig. 2. The crystal data and refinement details are found in Table 1, whereas selected bond lengths and bond angles are provided in Table 2. The asymmetric unit of the N-(4-chlorophenyl)-4-(dibenzo[*b,f*][1,4]thiazepin-11-yl)piperazine-1-carboxamide (**3h**) contains two separate molecular components, with

Table 2
Selected bond lengths [Å] and angles (°) for compound **3h**.

Bond lengths [Å]	**3h**	Bond lengths [Å]	**3h**
S(1)-C(13)	1.773 (3)	N(4)-C(12)	1.408 (4)
S(1)-C(20)	1.779 (4)	N(5)-C(33)	1.470 (4)
S(2)-C(40)	1.781 (4)	N(5)-C(34)	1.378 (5)
S(2)-C(41)	1.779 (4)	N(5)-C(47)	1.469 (5)
O(1)-C(8)	1.230 (4)	O(2)-C(31)	1.237 (4)
N(1)-C(34)	1.286 (5)	N(6)-C(11)	1.368 (5)
N(1)-C(35)	1.390 (4)	N(6)-C(18)	1.453 (4)
N(2)-C(7)	1.431 (5)	C(30)-N(7)	1.431 (5)
N(2)-C(8)	1.363 (4)	N(7)-C(31)	1.340 (5)
N(3)-C(8)	1.367 (5)	C(31)-N(8)	1.357 (5)
N(3)-C(9)	1.469 (4)	N(8)-C(32)	1.460 (4)
N(3)-C(19)	1.457 (4)	N(8)-C(48)	1.479 (5)
N(4)-C(11)	1.280 (5)		
Bond angles [°]	**3h**	Bond angles [°]	**3h**
C(13)-S(1)-C(20)	95.04 (18)	S(1)-C(13)-C(12)	120.4 (3)
C(40)-S(2)-C(41)	96.40 (18)	S(1)-C(13)-C(14)	119.8 (3)
C(34)-N(1)-C(35)	123.5 (3)	N(6)-C(18)-C(19)	110.7 (3)
C(7)-N(2)-C(8)	119.8 (3)	N(3)-C(19)-C(18)	110.8 (3)
C(8)-N(3)-C(9)	124.2 (3)	C(29)-C(30)-N(7)	120.0 (3)
C(8)-N(3)-C(19)	116.4 (3)	N(7)-C(30)-C(39)	120.6 (3)
C(9)-N(3)-C(19)	114.0 (3)	C(30)-N(7)-C(31)	120.7 (3)
C(11)-N(4)-C(12)	122.4 (3)	O(2)-C(31)-N(7)	120.5 (3)
C(33)-N(5)-C(34)	117.6 (3)	O(2)-C(31)-N(8)	122.0 (3)
C(33)-N(5)-C(47)	109.5 (3)	N(7)-C(31)-N(8)	117.5 (3)
C(34)-N(5)-C(47)	118.3 (3)	C(31)-N(8)-C(32)	126.2 (3)
N(2)-C(7)-C(6)	119.3 (3)	C(31)-N(8)-C(48)	118.1 (3)
N(2)-C(7)-C(17)	122.5 (4)	C(32)-N(8)-C(48)	111.9 (3)
O(1)-C(8)-N(2)	120.3 (3)	N(8)-C(32)-C(33)	110.0 (3)
O(1)-C(8)-N(3)	121.5 (3)	N(1)-C(34)-N(5)	119.5 (3)
N(2)-C(8)-N(3)	118.2 (3)	N(1)-C(34)-C(46)	125.8 (3)
N(3)-C(9)-C(10)	112.0 (3)	N(5)-C(34)-C(46)	114.5 (3)
C(10)-N(6)-C(11)	121.4 (3)	N(1)-C(35)-C(36)	118.6 (3)
C(10)-N(6)-C(18)	111.4 (3)	N(1)-C(35)-C(40)	123.5 (3)
C(11)-N(6)-C(18)	122.8 (3)	S(1)-C(40)-C(3)	119.8 (3)
N(4)-C(11)-N(6)	119.6 (3)	S(1)-C(40)-C(35)	120.1 (3)
N(4)-C(11)-C(25)	125.6 (3)	S(2)-C(41)-C(42)	120.8 (3)
N(6)-C(11)-C(25)	114.2 (3)	S(2)-C(41)-C(46)	119.3 (3)
N(4)-C(12)-C(13)	124.2 (3)	N(5)-C(47)-C(48)	110.8 (3)
N(4)-C(12)-C(27)	117.7 (3)		

different conformations. X-ray structure reveals that both these components are nonplanar. There are no lattice-held water molecules or organic solvent molecules in the unit cells of the determined structures. The Cl groups are coplanar with the attached benzene rings which are nearly antiparallel to the other benzene rings. The C—C—C bond angles in the aromatic ring are close to 120°, thus suggesting that the carbon atoms are sp^2 hybridized. The C—C bond distances in the aromatic rings are in the normal range of 1.34–1.51 Å, which is characteristic of delocalized aromatic rings. The molecular packing diagram shows four layers of molecules, which are independently arrange in the unit cell. Molecules forming each layer are connected through the intermolecular hydrogen bonding formed between NH and C=O. In each layer, the molecules are alternatively parallel.

2.4. Antimicrobial activity

All newly synthesized compounds (**3a-q**) were screened against standard one Gram-positive, *i.e.*, *S. aureus* and four Gram-negative, *i.e.*, *E. coli, P. aeruginosa, K. pneumonia and A. baumannii* bacterial strains. In addition, all these compounds were also screened against two fungal strains of *C. albicans* and *C. neoformans*. The results of the *in-vitro* antimicrobial activity are summarized in Table 3. In regard to *P. aeruginosa* and *A. baumannii,* the *in vitro* assay results, from all piperazine derivatives (**3a-q**), showed poor or even no growth inhibition (Table 3) indicating that cell impermeability could be the cause.

On the other hand, it was observed that all piperazine derivatives (**3a-q**) showed medium to good growth inhibition (Table 3) against Gram-negative bacteria *E. coli.* The increased growth inhibition is

Table 3
Antimicrobial activity of compounds (**3a–q**) with the concentration set at 32 μg/mL in DMSO.

	Percentage of inhibition of antibacterial and antifungal growth[a]						
	Antibacterial activity					Antifungal activity	
	Gram-positive	Gram-negative bacteria					
Compound (#)	*Staphylococcus aureus*	*Escherichia coli*	*Pseudomonas aeruginosa*	*Klebsiella pneumoniae*	*Acinetobacter baumannii*	*Candida albicans*	*Cryptococcus neoformans*
3a	12 ± 4	18 ± 2	3 ± 4	14 ± 8	8 ± 18	5 ± 4	−18 ± 1
3b	−4 ± 5	12 ± 2	−5 ± 2	−1 ± 8	**13 ± 3**	**12 ± 1**	−7 ± 4
3c	−18 ± 32	19 ± 1	6 ± 6	−8 ± 12	−35 ± 29	4 ± 4	**23 ± 12**
3d	11 ± 6	17 ± 8	−8 ± 4	5.4 ± 0.1	−2 ± 15	4 ± 4	−1 ± 3
3e	5 ± 3	**26 ± 3**	**9.0 ± 0.1**	**15 ± 6**	4 ± 6	4 ± 3	**12 ± 10**
3f	8 ± 1	20 ± 3	−5 ± 5	11 ± 2	9 ± 3	6 ± 1	0 ± 1
3g	7 ± 4	6 ± 2	−3 ± 0.4	−9 ± 3	−14 ± 2	**30 ± 8**	−8 ± 2
3h	7 ± 4	9 ± 2	−6 ± 1	−3 ± 4	−19 ± 13	7 ± 3	−31 ± 13
3i	7 ± 8	18 ± 2	3.7 ± 0.1	12 ± 1	−2 ± 8	3 ± 7	–22 ± 7
3j	**14 ± 6**	19 ± 2	−3 ± 2	10 ± 10	3 ± 3	1 ± 1	−4 ± 8
3k	10 ± 2	17.1 ± 0.2	−1 ± 1	**17 ± 2**	9 ± 9	−0.8 ± 0.1	−12 ± 3
3l	13 ± 6	13 ± 2	−3 ± 2	4 ± 2	−31 ± 2	5 ± 2	−26 ± 16
3m	−2 ± 4	17 ± 3	−2.1 ± 0.2	10 ± 2	6 ± 17	2 ± 6	9 ± 5
3n	−12 ± 28	14 ± 2	−1 ± 2	−6 ± 9	−42 ± 31	5 ± 6	**24 ± 6**
3o	7 ± 4	**25 ± 2**	3 ± 1	4 ± 8	4 ± 16	5 ± 4	9 ± 10
3p	8 ± 2	18 ± 2	2 ± 5	11 ± 4	7 ± 8	6 ± 7	−8 ± 2
3q	**14 ± 4**	11 ± 3	−1 ± 6	−2 ± 5	−28 ± 9	4 ± 3	−2 ± 6

[a] Highest percentile of antibacterial/antifungal growth inhibition are highlighted in bold. Data are expressed as the mean ± SD. SD = Standard Deviation.

presumably due to easy penetration of compounds into the lipid membranes of these organism. Regarding Gram positive bacteria *S. aureus,* compounds (**3a, 3d-l**, and **3o-q)** exhibited medium growth inhibition. Likewise, compounds (**3a**, **3e**, **3f**, **3i**, **3k**, and **3p**) showed medium growth inhibition against *K. pneumonia.* Also, compound (**3g**) exhibited very good growth inhibition (30.15%) towards *C. albicans* fungal strain, whereas (**3a-f**) and (**3h-3q**) showed moderate growth inhibition. Regarding fungal strain *C. neoformans,* piperazine derivatives **3c**, **3e**, **3m**, **3n**, and **3o** displayed medium to good growth inhibition while remaining adducts; **3a**, **3b**, **3d**, **3f-l**, and **3p-q** did not show any growth inhibition.

2.5. Molecular docking studies

To understand the mechanism of anti-microbial activity of the synthesized compounds, molecular modelling and docking studies were performed on the X-ray crystal structure of *E. coli* 24 kDa domain in complex with clorobiocin (PDB code: 1KZN; resolution 2.30 Å) using Surflex-Dock programme of Sybyl-X software. All 17 inhibitors were docked into the active site of the enzyme as shown in Fig. 3(A and B). The predicted binding energies of the compounds are listed in Table 4. The docking study revealed that all the compounds exhibited very good docking scores against *E. coli*.

Clorobiocin [Fig. 4(A–C)] was found to have hydrogen bonding interactions with ASP73 (2.04 Å; 3.72 Å), ASN46 (1.72 Å; 2.29 Å; 2.67 Å) and ARG136 (2.49 Å; 1.91 Å; 2.52 Å). As depicted in Fig. 5(A–C), compound **3e** makes two hydrogen bonding interactions at the active site of the enzyme (PDB ID: 1KZN), one interaction was the oxygen atom of carbonyl group with hydrogen of THR165 (−C═O···H-THR165, 2.31 Å) and remaining another hydrogen bonding interaction raised from the hydrogen atom of CONH group with oxygen of ASP73 (NH···O-ASP73, 2.00 Å). As depicted in Fig. 6(A–C), compound **3c**, makes three hydrogen bonding interactions at the active site of the enzyme (PDB ID: 1KZN). Among those, two interactions were of oxygen atom of carbonyl group with hydrogen atoms of THR165 and GLY77 (C═O···H-THR165, 2.66 Å; C═O···H-GLY77, 2.59 Å) and the remaining another hydrogen bonding interaction raised from the hydrogen atom of CONH group with oxygen of ASP73 (NH···O-ASP73, 2.06 Å). Fig. 7(A and B) represents the hydrophobic and hydrophilic amino acids surrounding compounds **3c** and **3e**.

All the compounds showed consensus score in the range 5.55–2.41, indicating the summary of all forces of interaction between ligands and the protein. These scores indicate that molecules preferentially bind to protein in comparison to the reference clorobiocin (Table 4). It was found that hydrogen bond formation with ASP73 amino acid residue may be responsible for the antibacterial activity compared to that observed for clorobiocin.

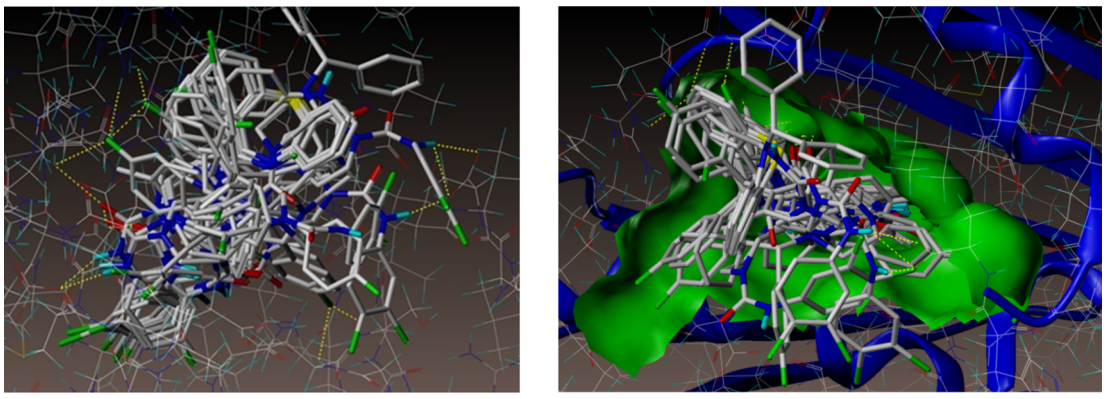

Fig. 3. Docked view of all compounds at the active site of the enzyme PDB ID: 1KZN.

Table 4
Surflex docking score (kcal/mol) of the piperazine derivatives for *E. coli* (PDB ID: 1KZN).

Mol. #	C Score[a]	Crash score[b]	Polar score[c]	D score[d]	PMF score[e]	G score[f]	Chem score[g]
Clorobiocin ligand	**12.14**	**−1.21**	**5.33**	**−189.513**	**−76.407**	**−135.711**	**−34.514**
3a	2.93	−0.87	0.00	−66.065	−20.007	−115.193	−16.162
3b	5.48	−1.69	1.46	−114.895	–23.772	−236.789	−25.490
3c	3.60	**−4.44**	1.32	−122.691	−18.028	−243.061	−24.762
3d	5.38	−0.62	0.96	−103.551	−31.084	−173.693	−27.155
3e	5.41	−1.77	0.64	**−128.063**	−12.168	−225.387	−24.369
3f	**5.54**	−1.99	0.92	−131.171	−12.123	−213.098	−24.211
3g	3.64	−0.82	0.05	−95.843	−8.012	−131.015	−19.207
3h	4.99	−0.61	1.04	−109.661	−35.048	−170.947	−27.589
3i	5.55	−2.28	1.33	−131.189	1.405	−231.666	**−30.644**
3j	2.72	−1.19	0.00	−93.647	8.001	−149.443	−15.933
3k	5.20	−1.39	0.00	−122.741	−1.386	−230.423	−21.916
3l	5.30	−0.76	1.11	−102.217	−28.486	−168.898	−26.264
3m	3.94	−3.38	0.04	−142.042	−6.368	**−245.636**	−26.355
3n	3.97	−1.02	1.46	−95.522	−7.291	−154.593	−21.745
3o	2.77	−2.56	0.00	−108.918	3.070	−145.135	−20.229
3p	2.41	−0.92	**1.82**	−77.155	−18.425	−101.856	−15.749
3q	5.24	−1.74	1.81	−123.589	**−36.455**	−205.531	−30.026

[a] CScore (Consensus Score) integrates a number of popular scoring functions for ranking the affinity of ligands bound to the active site of a receptor and reports the output of total score.
[b] Crash-score revealing the inappropriate penetration into the binding site. Crash scores close to 0 are favorable. Negative numbers indicate penetration.
[c] Polar indicating the contribution of the polar interactions to the total score. The polar score may be useful for excluding docking results that make no hydrogen bonds.
[d] D-score for charge and van der Waals interactions between the protein and the ligand.
[e] PMF-score indicating the Helmholtz free energies of interactions for protein–ligand atom pairs (Potential of Mean Force, PMF).
[f] G-score showing hydrogen bonding, complex (ligand–protein), and internal (ligand–ligand) energies.
[g] Chem-score points for H-bonding, lipophilic contact, and rotational entropy, along with an intercept term.

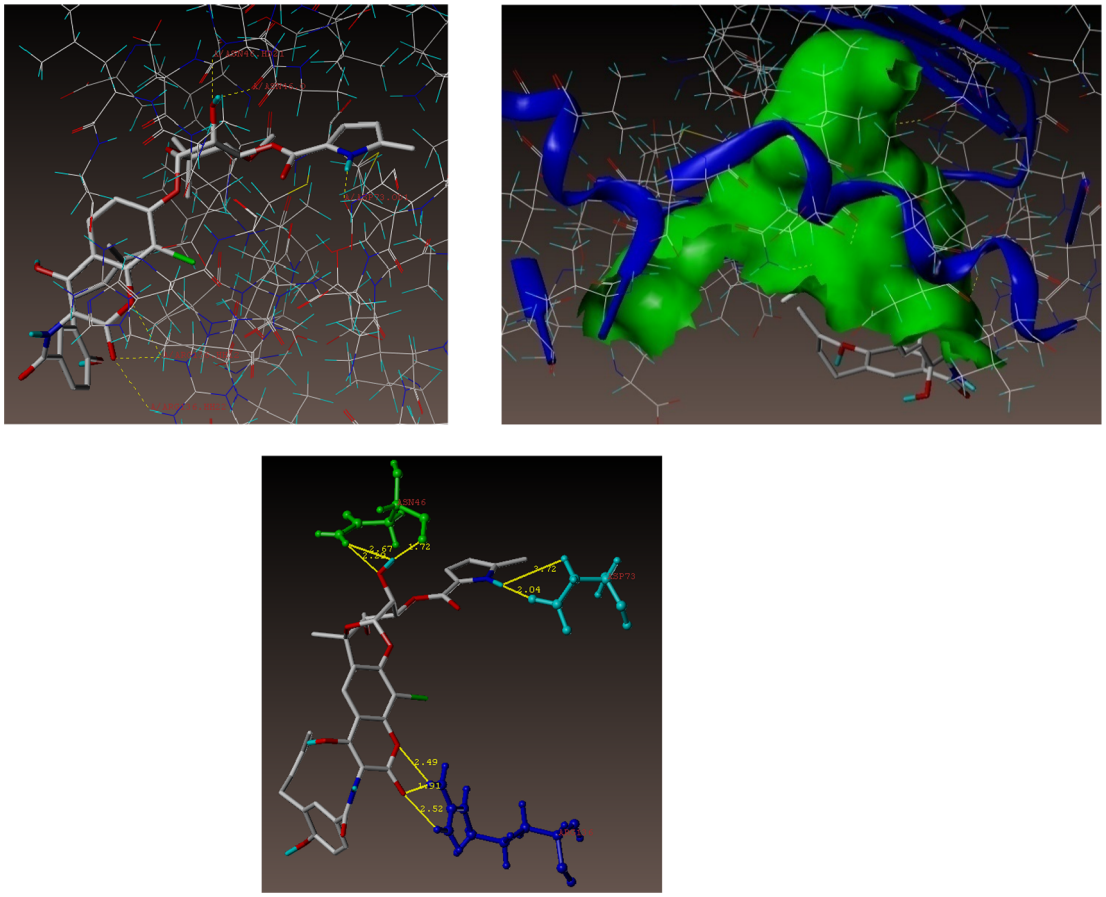

Fig. 4. Docked view of Clorobiocin at the active site of the enzyme PDB ID: 1KZN.

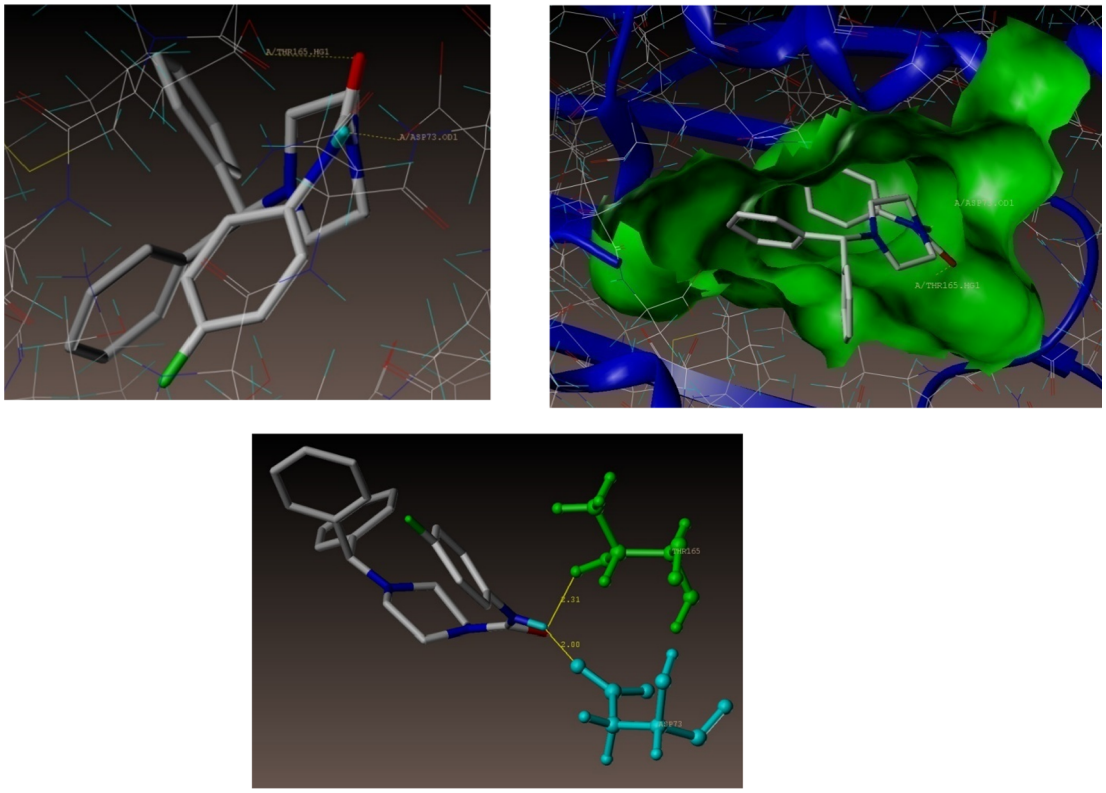

Fig. 5. Interaction of compound **3e** at the binding site of enzyme (PDB ID: 1KZN).

3. Conclusion

In summation, we have designed and synthesized a new series of piperazine derivatives containing bisaryl/thiazepine moieties. The structures of all molecules were confirmed through IR, ^{1}H NMR, ^{13}C NMR, and mass spectroscopy. In addition, the chemical structure of compound **3h** was clearly confirmed by single crystal X-ray diffraction analysis. All piperazine derivatives were screened for anti-microbial properties. In general, based on the biological evaluation results, compound **3e** showed the best inhibition of antimicrobial growth towards the bacteria and fungi strains evaluated. Additionally, gram-negative bacteria were also most inhibited with **3e**. Finally, the molecular

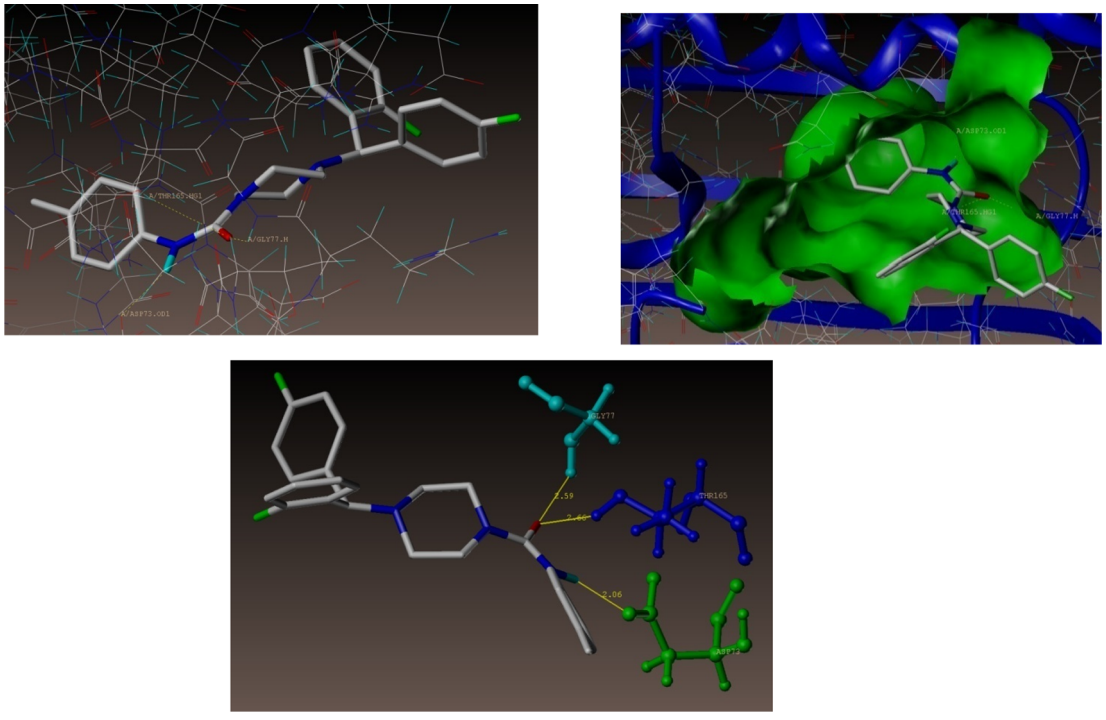

Fig. 6. Interaction of compound **3c** at the binding site of enzyme (PDB ID: 1KZ).

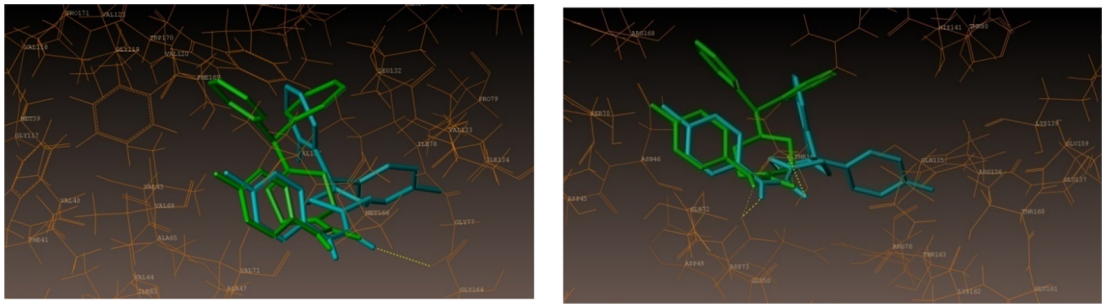

Fig. 7. A) Hydrophobic amino acids surrounded to compounds **3c** (cyan color) and **3e** (green color)). B) Hydrophilic amino acids surrounded **3c** and **3e**.

docking studies of all prepared molecules were carried out and the results revealed that all the piperazine derivatives showed very good docking score against *E coli*.

4. Experimental section: materials and methods

4.1. General considerations

All chemicals, including isocyanates, were procured commercially from Sigma-Aldrich chemical company and were used without further purification. All solvents purchased were of analytical grade and were used without further purification. All reactions were carried out under aerobic conditions, in oven-dried glassware, with magnetic stirring. Heating was accomplished by either a heating mantle or silicone oil bath. Reactions were monitored by thin-layer chromatography (TLC) performed on 0.25 mm Merck TLC silica gel plates, using UV light as a visualizing agent. Purification of reaction products was carried out by flash column chromatography using silica gel 60 (230–400 mesh). Yields refer to chromatographically pure material. Concentration in vacuo refers to the removal of volatile solvent, using a rotary evaporator attached to a dry diaphragm pump (10–15 mm Hg), followed by pumping to a constant weight with an oil pump (< 300 mTorr). ^{1}H NMR spectra were recorded on a JEOL Eclipse Plus 500 (500 MHz), and are reported relative to $CDCl_3$ (δ 7.26) or DMSO-d_6 (δ 2.50). ^{1}H NMR coupling constants (J) are reported in Hertz (Hz) and multiplicities are indicated as follows: s (singlet), d (doublet), t (triplet), quint (quintet), m (multiplet). Proton-decoupled ^{13}C NMR spectra were recorded on JEOL Eclipse Plus 500 (125 MHz) and reported relative to $CDCl_3$ (δ 77.00) or DMSO-d_6 (δ 39.52). X-ray diffraction data for compound (**3h**) was collected using Mo-Kα radiation and a Bruker SMART APEXII diffractometer [15]. The structure was solved by direct method using SHELXS-97 and refined by full-matrix least-squares on F2 for all data using SHELXL-97 at 100 K [21]. An analytical absorption correction, based on the shape of the crystal, was performed. All hydrogen atoms were added at calculated positions and refined using a riding model. Anisotropic thermal displacement parameters were used for all non-hydrogen atoms. Additional details involving data collection and reliability factors are listed in Table 1. CCDC 1,939,260 (for **3h**), contain the supplementary crystallographic data for this paper. These data can be obtained free of charge from the Cambridge Crystallographic Data Centre via http://www.ccdc.cam.ac.uk/data_request/cif.

4.2. Synthesis

4.2.1. General experimental procedure for synthesis of piperazine derivatives

To a solution of isocyanate (1.877 mmol) in toluene (2.5 mL) was added a solution of a monosubstituted piperazine (1.877 mmol) in toluene (1.0 mL). The reaction mixture was heated at 40–45 °C for 30 to 60 min. The reaction mixture was then cooled down to room temperature (22–25 °C) and the resulting solids were filtered and washed with more toluene (2.0 mL). The wet solids were then placed in 2.0 mL of toluene, stirred at room temperature for about 30 min, filtered and washed with toluene (1.0 mL) to obtain the crude disubstituted piperazine derivative. Finally, all crude derivatives were purified by silica-gel column chromatography using a mixture of dichloromethane/methanol (9:1) to afford pure piperazines products.

*4.2.1.1. Synthesis of 4-benzhydryl-N-(p-tolyl)piperazine-1-carboxamide **(3a)***. Compound (**3a**) was synthesized from 4-methyl phenyl isocyanate (0.25 g, 1.877 mmol) and 1-benzhydrylpiperazine (0.473 g, 1.877 mmol) according to the general procedure. White solid. Yield: 78% (0.56 g).^{1}H NMR ($CDCl_3$, 500 MHz) δ 7.43 (d, J = 7.5 Hz, 4H), 7.30 (t, J = 7.5 Hz, 4H), 7.22–7.19 (m, 4H), 7.06 (d, J = 8.0 Hz, 2H), 6.33(s, 1H), 4.25 (s, 1H), 3.47 (t, J = 4.5 Hz, 4H), 2.42 (t, J = 4.5 Hz, 4H), 2.29 (s, 3H). ^{13}C NMR ($CDCl_3$, 125 MHz) δ 155.2, 142.2, 136.3, 132.6, 129.3, 128.6, 127.8, 127.1, 75.9, 51.5, 44.2, 20.7.IR (KBr): $\bar{\upsilon}$ = 3257.05, 2952.2, 2810.92, 1637.37, 1598.01, 1287.71, 809.10. LC-MS for $C_{25}H_{27}N_3O$: m/z = 386 $[M + H]^+$.

*4.2.1.2. Synthesis of 4-((4-fluorophenyl)(phenyl)methyl)-N-(p-tolyl) piperazine-1-carboxamide **(3b)***. Compound (**3b**) was synthesized from 4-methylphenyl isocyanate (0.25 g, 1.877 mmol) and 1-((4-fluorophenyl)(phenyl)methyl)piperazine (0.50 g, 1.877 mmol) according to the general procedure. White solid. Yield: 74%, (0.56 g).^{1}H NMR ($CDCl_3$, 500 MHz) δ 7.40–7.38 (m, 4H), 7.30 (t, J = 7.0 Hz, 2H), 7.23–7.19 (m, 3H), 7.06 (d, J = 8.0 Hz, 2H), 6.99 (t, J = 8.5 Hz, 2H), 6.39 (s, 1H), 4.24 (s, 1H), 3,46 (t, J = 4.5 Hz, 4H), 2.41–2.39 (m, 4H), 2.29 (s, 3H). ^{13}C NMR ($CDCl_3$, 125 MHz) δ 161.8 (d, $^{1}J_{C,F}$ = 244.4 Hz), 155.2, 141.9, 138.0, 136.3, 132.6, 129.3, 129.2, 127.7, 127.2, 120.2, 115.5, 115.3, 75.1, 51.4, 44.1, 20.7. IR (KBr): $\bar{\upsilon}$ = 3313.58, 2790.2, 2948.15, 1637.09, 1515.01, 1237.92, 813.40. LC-MS for $C_{25}H_{26}FN_3O$: m/z = 404 $[M + H]^+$.

*4.2.1.3. Synthesis of 4-((2-fluorophenyl)(4-fluorophenyl)methyl)-N-(p-tolyl)piperazine-1-carboxamide **(3c)***. Compound (**3c**) was synthesized from 4-methylphenyl isocyanate (0.25 g, 1.877 mmol) and 1-((2-fluorophenyl)(4-fluorophenyl)methyl)piperazine (0.54 g, 1.877 mmol) according to the general procedure. White solid. Yield: 70% (0.55 g). ^{1}H NMR ($CDCl_3$, 500 MHz) δ 7.58 (t, J = 7.0 Hz, 1H), 7.42–7.39 (m, 2H), 7.20 (d, J = 8.5 Hz, 3H), 7.13 (t, J = 7.5 Hz, 1H), 7.05 (d, J = 8.0 Hz, 2H), 6.99 (t, J = 8.5 Hz, 3H), 6.41 (s, 1H), 4.70 (s, 1H), 3.46 (t, J = 4.5 Hz, 4H), 2.45–2.38 (m, 4H), 2.29 (s, 3H). ^{13}C NMR ($CDCl_3$, 125 MHz) δ 161.9 (d, $^{1}J_{C,F}$ = 244.4 Hz), 160.5 (d, $^{1}J_{C,F}$ = 244.4 Hz), 155.2, 136.9, 136.3, 132.7, 129.5 (d, $^{3}J_{C,F}$ = 8.4 Hz), 129.3, 128.8, 128.7, 128.5 (d, $^{3}J_{C,F}$ = 8.4 Hz), 128.4, 124.4, 120.3, 115.7, 115.4 (d, $^{2}J_{C,F}$ = 21.4 Hz), 65.9, 51.3, 44.1, 20.7. IR (KBr): $\bar{\upsilon}$ = 3265.25, 2810.19, 2952.8, 1634.57, 1508.80, 1249.81, 811.38. LC-MS for $C_{25}H_{25}F_2N_3O$: m/z = 422 $[M + H]^+$.

*4.2.1.4. Synthesis of 4-(dibenzo[b,f][1,4] thiazepin-11-yl)-N-(p-tolyl) piperazine-1-carboxamide **(3d)***. Compound (**3d**) was synthesized from 4-methylphenyl isocyanate (0.25 g, 1.877 mmol) and 11-piperazin-1-yl-dibenzo [*b,f*][1,4]thiazepine (0.55 g, 1.877 mmol) according to the

general procedure. White solid. Yield = 76% (0.61 g). ^{1}H NMR (DMSO-d_6, 500 MHz) δ 8.50 (s, 1H), 7.57–7.56 (m, 1H), 7.49–7.43 (m, 3H), 7.40–7.38 (m, 1H), 7.34 (d, J = 8.5 Hz, 2H), 7.22–7.16 (m, 1H), 7.05–7.03 (m, 3H), 6.91 (td, J = 7.5, 1.0 Hz, 1H), 3.60–3.47 (m, 8H), 2.23 (s, 3H). ^{13}C NMR (DMSO-d_6, 125 MHz) δ 160.1, 155.2, 148.5, 138.7, 137.8, 133.5, 132.1, 132.0, 131.4, 130.7, 129.3, 129.1, 129.0, 128.9, 128.8, 127.2, 125.1, 122.7, 119.9, 43.4, 20.4. IR (KBr): $\bar{\upsilon}$ = 3251.4, 2849.73, 2916.4, 1638.69, 1513.45, 1250.15, 810.81. LC-MS for $C_{25}H_{24}N_4OS$: m/z = 429 $[M + H]^+$.

*4.2.1.5. Synthesis of 4-benzhydryl-N-(4-chlorophenyl) piperazine-1-carboxamide (**3e**)*. Compound (**3e**) was synthesized from 4-chloro phenyl isocyanate (0.25 g, 1.627 mmol) and 1-benzhydrylpiperazine (0.41 g, 1.627 mmol) according to the general procedure. White solid. Yield = 75% (0.495 g). ^{1}H NMR (DMSO-d_6, 500 MHz) δ 8.60 (s, 1H), 7.48 (dt, J = 9.0, 2.5 Hz, 2H), 7.44 (d, J = 7.5 Hz, 4H), 7.30 (t, J = 7.5 Hz, 4H), 7.25 (dt, J = 9.5, 2.5 Hz, 2H), 7.19 (t, J = 7.5 Hz, 2H), 4.34 (s, 1H), 3.46 (t, J = 4.5 Hz, 4H), 2.32 (t, J = 4.0 Hz, 4H). ^{13}C NMR (DMSO-d_6, 125 MHz) δ 154.7, 142.5, 139.5, 128.6, 128.1, 127.6, 127.0, 125.3, 121.0, 74.8, 51.4, 43.8. IR (KBr): $\bar{\upsilon}$ = 3298.40, 2793.08, 2954.76, 1635.53, 1529.81, 1240.67, 821.77. LC-MS for $C_{24}H_{24}ClN_3O$: m/z = 406 $[M + H]^+$.

*4.2.1.6. Synthesis of N-(4-chlorophenyl)-4-((4-fluorophenyl)(phenyl) methyl)piperazine-1-carboxamide (**3f**)*. Compound (**3f**) was synthesized from 4-chloro phenyl isocyanate (0.25 g, 1.627 mmol) and 1-((4-fluorophenyl) (phenyl)methyl)piperazine (0.44 g, 1.627 mmol) according to the general procedure. White solid. Yield = 71% (0.49 g). ^{1}H NMR (DMSO-d_6, 500 MHz) δ 8.67 (s, 1H), 7.50–7.41 (m, 6H), 7.31 (t, J = 7.0 Hz, 2H), 7.25 (d, J = 9.0 Hz, 2H), 7.20 (t, J = 7.5 Hz, 1H), 7.13 (t, J = 8.0 Hz, 2H), 4.38 (s, 1H), 3.47 (s, 4H), 2.30 (s, 4H). ^{13}C NMR (DMSO-d_6, 125 MHz) δ 161.07 (d, $^1J_{C,F}$ = 240.9 Hz), 154.7, 142.3, 139.6, 138.7, 129.5 (d, $^3J_{C,F}$ = 8.4 Hz), 128.6, 128.1, 127.6, 127.0, 125.2, 121.0, 115.3 (d, $^2J_{C,F}$ = 20.3 Hz), 73.7, 51.3, 43.8. IR (KBr): $\bar{\upsilon}$ = 3305.20, 2791.24, 2955.9, 1634.24, 1504.97, 1282.91, 829.67. LC-MS for $C_{24}H_{23}ClFN_3O$: m/z = 424 $[M + H]^+$.

*4.2.1.7. Synthesis of N-(4-chlorophenyl)-4-((2-fluorophenyl)(4-fluorophenyl)methyl)piperazine-1-carboxamide (**3g**)*. Compound (**3g**) was synthesized from 4-chlorophenyl isocyanate (0.25 g, 1.627 mmol) and 1-((2-fluorophenyl)(4-fluorophenyl)methyl)piperazine (0.469 g, 1.627 mmol) according to the general procedure. White solid. Yield = 70% (0.50 g). ^{1}H NMR ($CDCl_3$, 500 MHz) δ 7.57 (t, J = 7.0 Hz, 1H), 7.40 (dd, J = 8.0, 6.0 Hz, 2H), 7.27–7.25 (m, 2H), 7.21–7.18 (m, 3H), 7.13 (t, J = 7.5 Hz, 1H), 6.99 (t, J = 8.5 Hz, 3H), 6.50 (s, 1H), 4.70 (s, 1H), 3.47 (t, J = 4.5 Hz, 4H), 2.46–2.39 (m, 4H). ^{13}C NMR ($CDCl_3$, 125 MHz) δ 161.1 (d, 1JC,F = 244.4 Hz), 160.6 (d, $^1J_{C,F}$ = 245.6 Hz), 154.7, 137.5, 136.8, 129.5 (d, $^3J_{C,F}$ = 7.1 Hz), 128.8, 128.6 (d, $^3J_{C,F}$ = 8.4 Hz), 128.4, 128.0, 124.4, 121.2, 115.8, 115.6, 115.4, 65.9, 51.2, 44.1. IR (KBr): $\bar{\upsilon}$ = 3264.76, 2818.08, 2951.4, 1640.27, 1508.64, 1280.07, 825.60. LC-MS for $C_{24}H_{22}ClF_2N_3O$: m/z = 442 $[M + H]^+$.

*4.2.1.8. Synthesis of N-(4-chlorophenyl)-4-(dibenzo[b,f][1,4]thiazepin-11-yl)piperazine-1-carboxamide (**3h**)*. Compound (**3h**) was synthesized from 4-chloro phenyl isocyanate (0.25 g, 1.627 mmol) and 11-Piperazin-1-yl-dibenzo [*b,f*][1,4] thiazepine (0.48 g, 1.627 mmol) according to the general procedure. White solid. Yield = 72% (0.526 g). ^{1}H NMR ($CDCl_3$, 500 MHz) δ 7.54 (d, J = 7.5 Hz, 1H), 7.41 (dd, J = 7.3, 1.0 Hz, 1H), 7.39–7.35 (m, 1H), 7.34–7.30 (m, 4H), 7.24–7.18 (m, 3H), 7.11 (dd, J = 8.0, 1.0 Hz, 1H), 6.93 (td, J = 7.5, 1.5 Hz, 1H), 6.65 (s, 1H), 3.73–3.48 (m, 8H). ^{13}C NMR ($CDCl_3$, 125 MHz) δ 160.7, 154.9, 140.0, 137.5, 133.6, 132.3, 132.2, 131.2, 129.2, 129.0, 128.9,128.8, 128.5, 128.2, 125.3, 123.5, 121.3, 43.6. IR (KBr): $\bar{\upsilon}$ = 3356, 2840.53, 2891.01, 1626.31, 1518.95, 1239.22, 803.49. LC-MS for $C_{24}H_{21}ClN_4OS$: m/z = 449 $[M + H]^+$.

*4.2.1.9. Synthesis of 4-benzhydryl-N-(4-fluorophenyl) piperazine-1-carboxamide (**3i**)*. Compound (**3i**) was synthesized from 4-fluorophenyl isocyanate (0.25 g, 1.823 mmol) and 1-benzhydrylpiperazine (0.46 g, 1.823 mmol) according to the general procedure. White solid. Yield = 77% (0.546 g). ^{1}H NMR ($CDCl_3$, 500 MHz) δ 7.42 (d, J = 7.0 Hz, 4H), 7.31–7.28 (m, 6H), 7.22–7.17 (m, 2H), 6.98–6.93 (m, 2H), 6.31 (s, 1H), 4.26 (s, 1H), 3.47 (s, 4H), 2.43 (s, 4H). ^{13}C NMR ($CDCl_3$, 125 MHz) δ 158.9 (d, $^1J_{C,F}$ = 240.8 Hz), 155.1, 142.1, 134.8, 128.6, 127.9, 127.2, 121.9 (d, $^3J_{C,F}$ = 8.4 Hz), 115.8 (d, $^2J_{C,F}$ = 22.6 Hz), 75.9, 51.5, 44.2. IR (KBr): $\bar{\upsilon}$ = 3302.39, 2794.53, 2951.98, 1630.84, 1510.68, 1287.08, 834.38. LC-MS for $C_{24}H_{24}FN_3O$: m/z = 390 $[M + H]^+$.

*4.2.1.10. Synthesis of N-(4-fluorophenyl)-4-((4-fluorophenyl)(phenyl) methyl)piperazine-1-carboxamide (**3j**)*. Compound (**3j**) was synthesized from 4-fluorophenyl isocyanate (0.25 g, 1.823 mmol) and 1-((4-fluorophenyl) (phenyl)methyl)piperazine (0.49 g, 1.823 mmol) according to the general procedure. White solid. Yield = 74% (0.549 g). ^{1}H NMR ($CDCl_3$, 500 MHz) δ 7.40–7.37 (m, 4H), 7.31–7.27 (m, 3H), 7.25–7.20 (m, 2H), 7.00–6.94 (m, 4H), 6.31 (s, 1H), 4.25 (s, 1H), 3.47 (t, J = 4.5 Hz, 4H), 2.42 (t, J = 3.0 Hz, 4H). ^{13}C NMR ($CDCl_3$, 125 MHz) δ 160.89, 158.9 (d, $^1J_{C,F}$ = 240.8 Hz), 155.1, 141.9, 137.9, 134.8, 129.3 (d, $^3J_{C,F}$ = 7.3 Hz), 128.7, 127.3, 122.0, 121.9, 115.5 (d, $^2J_{C,F}$ = 21.4 Hz), 115.4 (d, $^2J_{C,F}$ = 22.6 Hz), 75.1, 51.4, 44.2. IR (KBr): $\bar{\upsilon}$ = 3311.8, 2793.8, 2951.8, 1633, 1509, 1209.9, 835.8. LC-MS for $C_{24}H_{23}F_2N_3O$: m/z = 408 $[M + H]^+$.

*4.2.1.11. Synthesis of N-(4-fluorophenyl)-4-((2-fluorophenyl)(4-fluorophenyl)methyl)piperazine-1-carboxamide (**3k**)*. Compound (**3k**) was synthesized from 4-fluorophenyl isocyanate (0.25 g, 1.823 mmol) and 1-((2-fluorophenyl)(4-fluorophenyl)methyl)piperazine (0.525 g, 1.823 mmol) according to the general procedure. White solid. Yield = 70% (0.543 g). ^{1}H NMR (DMSO-d_6, 500 MHz) δ 8.55 (s, 1H), 7.64 (t, J = 7.0 Hz, 1H), 7.46–7.43 (m, 4H), 7.29–7.21 (m, 2H), 7.17–7.11 (m, 3H), 7.05 (t, J = 9.0 Hz, 2H), 4.71 (s, 1H), 3.47 (s, 4H), 2.35–2.28 (m, 4H). ^{13}C NMR (DMSO-d_6, 125 MHz) δ 160.2, 160.0 (d, 1JC,F = 242.0 Hz), 158.3, 156.4, 155.0, 137.2, 136.8, 129.7, 128.9, 128.7, 124.8, 121.4, 121.3, 115.7, 115.4 (d, $^2J_{C,F}$ = 21.5 Hz), 114.8 (d, $^2J_{C,F}$ = 22.6 Hz), 65.7, 51.2, 43.8. IR (KBr): $\bar{\upsilon}$ = 3307, 2814.18, 1628.47, 1506.23, 1223.83, 816.77. LC-MS for $C_{24}H_{22}F_3N_3O$: m/z = 426 $[M + H]^+$.

*4.2.1.12. Synthesis of 4-(dibenzo[b,f][1,4] thiazepin-11-yl)-N-(4-fluorophenyl)piperazine-1-carboxamide (**3l**)*. Compound (**3l**) was synthesized from 4-fluorophenyl isocyanate (0.25 g, 1.823 mmol) and 11-piperazin-1-yl-dibenzo [*b,f*][1,4]thiazepine (0.538 g, 1.823 mmol) according to the general procedure. White solid. Yield = 71% (0.56 g). ^{1}H NMR (DMSO-d_6, 500 MHz) δ 8.64 (s, 1H), 7.58–7.55 (m, 1H), 7.49–7.45 (m, 5H), 7.39 (dd, , J = 7.5, 2.0 Hz, 1H), 7.20 (td, J = 7.5, 1.0 Hz, 1H), 7.11–7.05 (m, 2H), 7.03 (dd, J = 7.8, 1.5 Hz, 1H), 6.91 (td, J = 7.5, 1.0 Hz, 1H), 3.61–3.39 (m, 8H). ^{13}C NMR (DMSO-d_6, 125 MHz) δ 160.1, 158.4, 156.5, 155.2, 148.5, 138.7, 136.7, 133.4, 132.1, 132.0, 131.4, 129.3, 129.1, 129.0, 128.2, 127.3, 125.1, 122.8, 121.5 (d, $^3J_{C,F}$ = 8.3 Hz), 114.8 (d, $^2J_{C,F}$ = 22.6 Hz), 43.4. IR (KBr): $\bar{\upsilon}$ = 3342.7, 2859.21, 2892.1, 1641.98, 1508.33, 1240.54, 812.81. LC-MS for $C_{24}H_{21}FN_4OS$: m/z = 433 $[M + H]^+$.

*4.2.1.13. Synthesis of 4-benzhydryl-N-(3,4-dichlorophenyl)piperazine-1-carboxamide (**3m**)*. Compound (**3m**) was synthesized from 3,4-dichlorophenyl isocyanate (0.25 g, 1.329 mmol) and 1-benzhydrylpiperazine (0.335 g, 1.329 mmol) according to the general procedure. White solid. Yield = 74% (0.433 g). ^{1}H NMR (DMSO-d_6, 500 MHz) δ 8.76 (s, 1H), 7.82 (d, J = 2.0 Hz, 1H), 7.46–7.41 (m, 6H), 7.3 (t, J = 8.0 Hz, 4H), 7.25–7.14 (m, 2H), 4.34 (s, 1H), 3.47 (t, J = 4.5 Hz, 4H), 2.33–2.29 (m, 4H). ^{13}C NMR (DMSO-d_6, 125 MHz) δ 154.4, 142.5, 140, 130.6, 130.1, 128.6, 127.6, 127.0, 122.9, 120.4,

119.2, 74.7, 51.3, 43.8. IR (KBr): $\bar{\upsilon}$ = 3258.54, 2814.75, 2953, 1642.66, 1505.68, 1245.13, 823.55. LC-MS for $C_{24}H_{23}Cl_2N_3O$: *m/z* = 441 $[M + H]^+$.

*4.2.1.14. Synthesis of N-(3,4-dichlorophenyl)-4-((4-fluorophenyl)(phenyl) methyl)piperazine-1-carboxamide (**3n**).* Compound (**3n**) was synthesized from 3,4-dichlorophenyl isocyanate (0.25 g, 1.329 mmol) and 1-((4-fluorophenyl) (phenyl)methyl)piperazine (0.36 g, 1.329 mmol) according to the general procedure. White solid. Yield = 76% (0.46 g). ^{1}H NMR (DMSO-d_6, 500 MHz) δ 8.83 (s, 1H), 7.83 (s, 1H), 7.47–7.41 (m, 6H), 7.31 (t, *J* = 7.5 Hz, 2H), 7.20 (t, *J* = 7.0 Hz, 1H), 7.13 (t, *J* = 8.5 Hz, 2H), 4.38 (s, 1H), 3.47 (s, 4H), 2.30 (s, 4H). ^{13}C NMR (DMSO-d_6, 125 MHz) δ 161.1 (d, $^1J_{C,F}$ = 240.9 Hz), 154.4, 142.2, 140.9, 138.6, 130.5, 130.1, 129.5 (d, $^3J_{C,F}$ = 8.4 Hz), 128.6, 127.6, 127.0, 122.8, 120.3, 119.2, 115.3 (d, $^2J_{C,F}$ = 21.4 Hz), 73.7, 51.2, 43.8. IR (KBr): $\bar{\upsilon}$ = 3301.2, 2791.11, 2952.46, 1637.27, 1505, 1239.68, 823.96. LC-MS for $C_{24}H_{22}Cl_2FN_3O$: *m/z* = 459 $[M + H]^+$.

*4.2.1.15. Synthesis of N-(3,4-dichlorophenyl)-4-((2-fluorophenyl)(4-fluorophenyl)methyl)piperazine-1-carboxamide (**3o**).* Compound (**3o**) was synthesized from 3,4-dichlorophenyl isocyanate (0.25 g, 1.329 mmol) and 1-((2-fluorophenyl) (4-fluorophenyl) methyl) piperazine (0.383 g, 1.329 mmol) according to the general procedure. White solid. Yield = 72% (0.456 g). ^{1}H NMR (DMSO-d_6, 500 MHz) δ 8.79 (s, 1H). 7.81 (d, *J* = 2.0 Hz, 1H), 7.65–7.62 (m, 1H), 7.46–7.41 (m, 4H), 7.29–7.21 (m, 2H), 7.17–7.11 (m, 3H), 4.71 (s, 1H), 3.47 (t, *J* = 4.5 Hz, 4H), 2.39–2.29 (m, 4H). ^{13}C NMR (DMSO-d_6, 125 MHz) δ 161.7 (d, $^1J_{C,F}$ = 240.9 Hz), 160.5 (d, $^1J_{C,F}$ = 243.3 Hz), 154.9, 141.4, 137.7, 131.1, 130.7, 130.2 (d, $^3J_{C,F}$ = 8.4 Hz), 129.5 (d, $^3J_{C,F}$ = 8.4 Hz), 129.2, 129.1, 125.3, 123.4, 120.9, 119.8, 116.3, 116.0 (d, $^2J_{C,F}$ = 20.3 Hz), 66.1, 51.6, 44.3. IR (KBr): $\bar{\upsilon}$ = 3267.2, 2815.5, 2953, 1640.51, 1507.84, 1244.97, 821.59. LC-MS for $C_{24}H_{21}Cl_2F_2N_3O$: *m/z* = 477 $[M + H]^+$.

*4.2.1.16. Synthesis of 4-(bis(4-fluorophenyl) methyl)-N-(3,4-dichlorophenyl)piperazine-1-carboxamide (**3p**).* Compound (**3p**) was synthesized from 3,4-dichlorophenyl isocyanate (0.25 g, 1.329 mmol) and 1-(bis(4-fluorophenyl) methyl)piperazine (0.383 g, 1.329 mmol) according to the general procedure. White solid. Yield = 75% (0.475 g). ^{1}H NMR (DMSO-d_6, 500 MHz) δ 8.77 (s, 1H), 7.81 (d, *J* = 2.5 Hz, 1H), 7.46–7.41 (m, 6H), 7.15–7.12 (m, 4H), 4.43 (s, 1H), 3.46 (t, *J* = 4.5 Hz, 4H), 2.29 (t, *J* = 4.5 Hz, 4H). ^{13}C NMR (DMSO-d_6, 125 MHz) δ 162.1, 160.2, 154.4, 140.9, 138.3, 130.6, 130.1, 129.5, 129.4, 122.9, 120.4, 119.2, 115.5, 115.3, 72.7, 51.1, 43.8. IR (KBr): $\bar{\upsilon}$ = 3305.63, 2789.71, 2952.67, 1637.30, 1505.19, 1235.69, 818.05. LC-MS for $C_{24}H_{21}Cl_2F_2N_3O$: *m/z* = 477 $[M + H]^+$.

*4.2.1.17. Synthesis of 4-(dibenzo[b,f][1,4]-thiazepin-11-yl)-N-(3,4-dichlorophenyl)piperazine-1-carboxamide (**3q**).* Compound (**3q**) was synthesized from 3,4-dichlorophenyl isocyanate (0.25 g, 1.329 mmol) and 11-piperazin-1-yl-dibenzo [*b,f*][1,4]thiazepine (0.392 g, 1.329 mmol) according to the general procedure. White solid. Yield = 73% (0.469 g). ^{1}H NMR ($CDCl_3$, 500 MHz) δ 7.58 (d, *J* = 2.0 Hz, 1H), 7.54 (d, *J* = 7.5 Hz, 1H), 7.41 (dd, *J* = 7.8, 1.0 Hz, 1H), 7.39–7.30 (m, 4H), 7.21–7.18 (m, 2H), 7.11 (dd, *J* = 8.0, 1.5 Hz, 1H), 6.93 (td, *J* = 7.8, 1.0 Hz, 1H), 6.70 (s, 1H), 3.63–3.49 (m, 8H). ^{13}C NMR ($CDCl_3$, 125 MHz) δ 160.7, 154.5, 140.0, 138.5, 133.6, 132.5, 132.4, 132.3, 131.3, 129.2, 128.9, 128.5, 126.2, 125.3, 123.5, 121.6, 119.2, 43.6. IR (KBr): $\bar{\upsilon}$ = 3239.58, 2870.6, 2898.6, 1632.92, 1503.66, 1243.45, 807.94. LC-MS for $C_{24}H_{20}Cl_2N_4OS$: *m/z* = 484 $[M + H]^+$.

4.3. Antimicrobial studies

Samples were prepared in DMSO and water to a final testing concentration of 32 μg/mL or 20 μM (unless otherwise indicated in the data sheet), in a 384-well, non-binding surface plate (NBS) for each bacterial/fungal strain, and in duplicate (n = 2), keeping the final DMSO concentration to a maximum of 1% DMSO [22–26]. All the sample preparations for antimicrobial studies where done using liquid handling robots.

4.3.1. Antimicrobial assay

Primary antimicrobial screening study via whole cell growth inhibition assays were carried out using compounds (**3a-q**) at a single concentration, in duplicate (n = 2). The inhibition of growth was measured against five bacteria: *Escherichia coli (E. coli) ATCC 25922*, *Klebsiella pneumonia (K. pneumoniae) ATCC 700603, Acinetobacter baumannii (A. Baumannii) ATCC 19606, Pseudomonas aeruginosa (P. Aeruginosa) ATCC 27853*) and *Staphylococcus aureus (S. aureus) ATCC 43300*, and two fungi: *Candida albicans (C. albicans) ATCC 90,028* and *Cryptococcus neoformans (C. Neoformans) ATCC 208,821* [27].

4.3.2. Procedure

All bacteria were cultured in Cation-adjusted Mueller Hinton broth (**CAMHB**) at 37 °C overnight. A sample of each culture was then diluted 40-fold in fresh broth and incubated at 37 °C for 1.5–3 h. The resultant mid-log phase cultures were diluted (CFU/mL measured by OD600), then added to each well of the compound containing plates, giving a cell density of 5x10^5 CFU/mL and a total volume of 50 μL. All plates were covered and incubated at 37 °C for 18 h without shaking.

4.3.3. Analysis

Inhibition of bacterial growth was determined measuring absorbance at 600 nm (OD600), using a Tecan M1000 Pro monochromator plate reader. The percentage of growth inhibition was calculated for each well, using the negative control (media only) and positive control (bacteria without inhibitors) on the same plate as references. The significance of the inhibition values was determined by modified Z-scores, calculated using the median and MAD of the samples (no controls) on the same plate. Samples with inhibition value above 80% and Z-Score above 2.5 for either replicate (n = 2 on different plates) were classed as actives. Samples with inhibition values between 50 and 80% and Z-Score above 2.5 for either replicate (n = 2 on different plates) were classed as partial actives.

4.3.4. Antifungal assay

4.3.4.1. Procedure. Fungi strains were cultured for 3 days on Yeast Extract-Peptone Dextrose (**YPD**) agar at 30 °C. A yeast suspension of 1×10^6–5×10^6 CFU/mL (as determined by OD530) was prepared from five colonies. The suspension was subsequently diluted and added to each well of the compound-containing plates giving a final cell density of fungi suspension of 2.5×10^3 CFU/mL and a total volume of 50 μL. All plates were covered and incubated at 35 °C for 24 h without shaking.

4.3.4.2. Analysis. Growth inhibition of *C. albicans* was determined measuring absorbance at 530 nm (OD530), while the growth inhibition of *C. neoformans* was determined measuring the difference in absorbance between 600 and 570 nm (OD600-570), after the addition of resazurin (0.001% final concentration) and incubation at 35 °C for additional 2 h. The absorbance was measured using a Biotek Synergy HTX plate reader. The percentage of growth inhibition was calculated for each well, using the negative control (media only) and positive control (fungi without inhibitors) on the same plate. The significance of the inhibition values was determined by modified Z-scores, calculated using the median and MAD of the samples (no controls) on the same plate. Samples with inhibition value above 80% and Z-Score above 2.5 for either replicate (n = 2 on different plates) were classed as actives. Samples with inhibition values between 50 and 80% and Z-Score above 2.5 for either replicate (n = 2 on different plates) were classed as partial actives.

4.4. Docking simulations

For the docking of ligands to protein active sites, and for estimating the binding affinities of docked compounds, Surflex-Dock module, a fully automatic docking tool available on Sybyl X-2.0version (Tripos Inc.), was used in this study [28]. Docking simulations: The X-ray Crystal Structure of *E. coli* 24 kDa Domain in Complex with clorobiocin (PDB code: 1KZN; resolution 2.30A; http://www. rcsb.org) was obtained from protein data bank in PDB format as starting point. Protein structure with all water molecules deleted was used for docking simulations. Mislabeled atom types from the pdb file were corrected, subsequently, proline F angles were fixed at 700 side chain amides were checked to maximize potential hydrogen bonding, side chains were checked for close van der Waals contacts, and essential hydrogens were added. The model was checked for conformational problems using the module ProTable from Sybyl. Ramachandran plot of the backbone torsion angles phi and psi, local geometry and the location of buried polar residues/exposed non-polar residues were examined. The protein was subjected to energy minimization following the gradient termination of the Powell method for 3000 iterations using Kollman united force field, with non-bonding cut-off set at 9.0 and the dielectric constant set at 4.0. Energy minimization for synthesized compounds, including clorobiocin, were carried out by the Powell method for 3000 iterations using Tripos force field and Gasteiger charge with non-bonding cut-off set at 9.0 and the dielectric constant set at 4.0. The synthesized compounds were docked to DNA gyrase subunit A (PDB code: 1KZN) using Surflex-Dock programme in Sybyl software by incremental construction approach of building the structure in the active site so as to favor the binding affinity. Finally, the docked ligands were ranked based on a variety of scoring functions that have been compiled into the single consensus score (C-score).

Acknowledgements

Florida Gulf Coast University and the University of Texas at Arlington partially supported this work. The ACS Petroleum Research Fund supported this research (grant # 58269-ND1). The authors also acknowledge Dr. Delphine Gout for X-ray data collection and UTA for additional instrumentation. The authors thank DST-Nanomission, India (SR/NM/NS-20/2014), DST-SERB, India [SERB/F/1423/2017–18 (File No. YSS/2015/000010)] and Jain University, India for financial support. Antimicrobial screening was performed by CO-ADD (The Community for Antimicrobial Drug Discovery), funded by the Welcome Trust (UK) and The University of Queensland (Australia).

Appendix A. Supplementary material

Supplementary data to this article can be found online at https://doi.org/10.1016/j.bioorg.2019.103217.

References

[1] M.K. Chattopadhyay, R. Chakraborty, H.-P. Grossart, G.S. Reddy, M.V. Jagannadham, Antibiotic resistance of bacteria, BioMed Res. Int. 2015 (2015) 2.
[2] J.M. Blair, M.A. Webber, A.J. Baylay, D.O. Ogbolu, L.J. Piddock, Molecular mechanisms of antibiotic resistance, Nat. Rev. Microbiol. 13 (2015) 42–51.
[3] D. Schillaci, V. Spanò, B. Parrino, A. Carbone, A. Montalbano, P. Barraja, P. Diana, G. Cirrincione, S. Cascioferro, Pharmaceutical approaches to target antibiotic resistance mechanisms, J. Med. Chem. 60 (2017) 8268–8297.
[4] V. Patil, E. Barragan, S.A. Patil, S.A. Patil, A. Bugarin, Direct synthesis and antimicrobial evaluation of structurally complex chalcones, ChemistrySelect 1 (2016) 3647–3650.
[5] M. Patil, A. Noonikara-Poyil, S.D. Joshi, S.A. Patil, S.A. Patil, A. Bugarin, Synthesis, molecular docking studies, and antimicrobial evaluation of new structurally diverse ureas, Bioorg. Chem. 87 (2019) 302–311.
[6] S. Patil, J. Claffey, A. Deally, M. Hogan, B. Gleeson, L.M. Menéndez Méndez, H. Müller-Bunz, F. Paradisi, M. Tacke, Synthesis, cytotoxicity and antibacterial studies of p-methoxybenzyl-substituted and benzyl-substituted n-heterocyclic carbene-silver complexes, Eur. J. Inorg. Chem. (2010) 1020–1031.
[7] S. Patil, A. Deally, B. Gleeson, H. Müller-Bunz, F. Paradisi, M. Tacke, Novel benzyl-substituted N-heterocyclic carbene–silver acetate complexes: synthesis, cytotoxicity and antibacterial studies, Metallomics 3 (2011) 74–88.
[8] S.A. Patil, S.A. Patil, R. Patil, Medicinal applications of (benz)imidazole- and indole-based macrocycles, Chem. Biol. Drug Des. 89 (2017) 639–649.
[9] S.A. Patil, S.A. Patil, R. Patil, R.S. Keri, S. Budagumpi, G.R. Balakrishna, M. Tacke, N-heterocyclic carbene metal complexes as bio-organometallic antimicrobial and anticancer drugs, Future Med. Chem. 7 (2015) 1305–1333.
[10] C.R. Shahini, G. Achar, S. Budagumpi, H. Müller-Bunz, M. Tacke, S.A. Patil, Benzoxazole and dioxolane substituted benzimidazole–based N–heterocyclic carbene–silver(I) complexes: synthesis, structural characterization and in vitro antimicrobial activity, J. Organomet. Chem. 868 (2018) 1–13.
[11] C.R. Shahini, G. Achar, S. Budagumpi, M. Tacke, S.A. Patil, Non–symmetrically p–nitrobenzyl–substituted N–heterocyclic carbene–silver(I) complexes as metallo-pharmaceutical agents, Appl. Organomet. Chem. 31 (2017) e3819.
[12] C.R. Shahini, G. Achar, S. Budagumpi, M. Tacke, S.A. Patil, Synthesis, structural investigation and antibacterial studies of non–symmetrically p–nitrobenzyl substituted benzimidazole N–heterocyclic carbene–silver(I) complexes, Inorg. Chim. Acta 466 (2017) 432–441.
[13] T.V. Subramanya Prasad, C.R. Shahini, S.A. Patil, X. Huang, A. Bugarin, S.A. Patil, Non-symmetrically p-nitrobenzyl- and p-cyanobenzyl-substituted N-heterocyclic carbene-silver(I) complexes: synthesis, characterization and antibacterial studies, J. Coord. Chem. 70 (2017) 600–614.
[14] G.G. Zhanel, A. Walkty, L. Vercaigne, J.A. Karlowsky, J. Embil, A.S. Gin, D.J. Hoban, The new fluoroquinolones: A critical review, Canad. J. Infect. Dis. = J. Canad. Malad. Infect. 10 (1999) 207–238.
[15] R.S. Upadhayaya, N. Sinha, S. Jain, N. Kishore, R. Chandra, S.K. Arora, Optically active antifungal azoles: synthesis and antifungal activity of (2R,3S)-2-(2,4-difluorophenyl)-3-(5-{2-[4-aryl-piperazin-1-yl]-ethyl}-tetrazol-2-yl/1-yl)-1-[1,2,4]-triazol-1-yl-butan-2-ol, Bioorg. Med. Chem. 12 (2004) 2225–2238.
[16] M.R. Gudisela, N. Srinivasu, C. Mulakayala, P. Bommu, M.V.B. Rao, N. Mulakayala, Design, synthesis and anticancer activity of N-(1-(4-(dibenzo[*b,f*][1,4]thiazepin-11-yl)piperazin-1-yl)-1-oxo-3-phenylpropan-2-yl derivatives, Bioorg. Med. Chem. Lett. 27 (2017) 4140–4145.
[17] S. Shivprakash, G.C. Reddy, Stereoselective Synthesis of (Z)-1-Benzhydryl-4-cinnamylpiperazines via the wittig reaction, Synth. Commun. 44 (2014) 600–609.
[18] Bruker, APEX2 and SAINT, Bruker AXS Inc., Madison, Wisconsin, USA, 2014.
[19] G. Sheldrick, A short history of SHELX, Acta Crystallogr. Sect. A: Found. Adv. 64 (2008) 112–122.
[20] V. Petříček, M. Dušek, L. Palatinus, Crystallographic computing system JANA2006: general features, Zeits. Kristallogr. – Crystall. Mater. 229 (2014) 345–352.
[21] G.M. Sheldrick, A short history of SHELX, Acta Crystallogr. Sect. A, Found. Crystall. 64 (2008) 112–122.
[22] A.R. Ahameethunisa, W. Hopper, Antibacterial activity of artemisia nilagirica leaf extracts against clinical and phytopathogenic bacteria, BMC Complement. Alternat. Med. 10 (2010) 6.
[23] M. Balouiri, M. Sadiki, S.K. Ibnsouda, Methods for in vitro evaluating antimicrobial activity: a review, J. Pharm. Anal. 6 (2016) 71–79.
[24] L. Forbes, K. Ebsworth-Mojica, L. DiDone, S.-G. Li, J.S. Freundlich, N. Connell, P.M. Dunman, D.J. Krysan, A high throughput screening assay for anti-mycobacterial small molecules based on adenylate kinase release as a reporter of cell lysis, PLoS ONE 10 (2015) e0129234.
[25] K.D. Greis, S. Zhou, R. Siehnel, C. Klanke, A. Curnow, J. Howard, G. Layh-Schmitt, Development and validation of a whole-cell inhibition assay for bacterial methionine aminopeptidase by surface-enhanced laser desorption ionization-time of flight mass spectrometry, Antimicrob. Agents Chemother. 49 (2005) 3428–3434.
[26] F. Nasrin, I.J. Bulbul, Y. Begum1, S. Khanum1, In vitro antimicrobial and cytotoxicity screening of n-hexane, chloroform and ethyl acetate extracts of Lablab purpureus (L.) leaves, Agric. Biol. J. N. Am. 3 (2012) 43–48.
[27] I.A. Edwards, A.G. Elliott, A.M. Kavanagh, J. Zuegg, M.A.T. Blaskovich, M.A. Cooper, Contribution of amphipathicity and hydrophobicity to the antimicrobial activity and cytotoxicity of β-hairpin peptides, ACS Infect. Dis. 2 (2016) 442–450.
[28] Tripos International, Sybyl-X 2.0, St. Louis, MO, USA, 2012.